ACADEMIC PRESS

Available online at www.sciencedirect.com

SCIENCE DIRECT®

Journal of Sound and Vibration 261 (2003) 421–441

JOURNAL OF SOUND AND VIBRATION

www.elsevier.com/locate/jsvi

Modified independent modal space control of m.d.o.f. systems

J.Q. Fang[a,*], Q.S. Li[b,1], A.P. Jeary[c]

[a] *Public Works & Government Services Canada, Pacific Region, 641-800 Burrard Street, Vancouver, BC, Canada V6Y 2V8*

[b] *Department of Building and Construction, City University of Hong Kong, Tat Chee Avenue, Kowloon, Hong Kong*

[c] *University of Western Sydney, School of Construction and Building Sciences, 39 Annangrove Road, Kenthurst, Sydney, NSW 2156, Australia*

Received 23 September 1997; accepted 22 May 2002

Abstract

The performance of the independent modal space control (IMSC) algorithm for structural vibration control is examined in this paper. Both the theoretical analysis and numerical simulation show that, for a multi-degree-of-freedom system, the modal control forces may increase the contributions of the vibration of higher modes (uncontrolled modes) to the system response if the IMSC algorithm is used to design a structural control system. Therefore, the responses of the controlled structure may be underestimated if the effects of control forces on the higher modes are not considered in the response analysis. A new control algorithm—modified independent modal space control (MIMSC) algorithm is proposed in this paper for eliminating the effect of modal control force on the uncontrolled modes. Numerical example shows that the structural responses can be effectively reduced when control system design is carried out based on the proposed algorithm. By comparing the simulated results obtained by the IMSC and MIMSC algorithms, it is found that, in order to achieve the same control objective, the proposed algorithm is more effective than IMSC since the modal control forces do not have any effect on the uncontrolled modes. In order to verify the effectiveness of the proposed algorithm, a practical example—active control design of UCLA Math-Science Building is presented and discussed.

1. Introduction

In recent years, great progress has been achieved in the field of active structural vibration control. A variety of control algorithms have been developed specifically for civil engineering structures [1–6] and significant full-scale active control systems have been installed in actual structures and have performed well for the purposes intended [7,8]. While significant progress has

*Corresponding author. UBC, Department of Mathematics, Vancouver, BC, Canada V6T 1Z2.
E-mail address: gfang@math.ubc.ca (J.Q. Fang).
[1] Also to be corresponded.

0022-460X/03/$ - see front matter
PII: S0022-460X(02)01085-4

been made, the true potential of active vibration control of structures has not been fully exploited. In this paper, the performance of the IMSC method, which is receiving intense interest in the control of multi-degree-of-freedom (m.d.o.f.) systems and has been successively applied to a wide variety of practical problems, is examined. Generally speaking, the IMSC method combines the modal decomposition with classical linear quadratic regulator (LQR) control law. The control gain for each of the modal controls can be found by solving a second order Riccati equation. The computational work can be reduced greatly if the IMSC algorithm is used to design the control system since the design is carried out based on the lower frequency modes. However, a recent study [9] demonstrates that, when control design is conducted based on the IMSC algorithm, the control forces may increase the contribution of the higher modes (uncontrolled modes) to the system responses. The purpose of this paper is to examine the effects of control forces on the uncontrolled modes and to propose an efficient algorithm to overcome the drawbacks of the IMSC algorithm.

The work presented in this paper contains two parts: firstly, by means of a theoretical analysis and a numerical simulation study, the effects of the control forces on the uncontrolled modes are investigated; secondly, a new control algorithm—modified independent modal space control (MIMSC) algorithm is proposed. Since there is no effect of the control forces on the uncontrolled modes, the control system designed by the proposed algorithm has higher control efficiency than those designed based on the IMSC algorithm. The results of the numerical simulation indicate that the implementation of the new control algorithm is simple and convenient, and its design can be carried out following the same procedure as in the IMSC case.

2. Independent modal space control algorithm

The vibration equation of a controlled MDOF system is

$$\mathbf{M}\ddot{\mathbf{z}}(t) + \mathbf{C}\dot{\mathbf{z}}(t) + \mathbf{K}\mathbf{z}(t) = \mathbf{D}\mathbf{u}(t) + \mathbf{F}(t), \tag{1}$$

where $\mathbf{M}$, $\mathbf{C}$, $\mathbf{K}$ are $n \times n$ mass, damping and stiffness matrices, respectively; $\mathbf{z}(t) = [z_1, z_2, \ldots, z_n]^{\mathrm{T}}$ is an n-dimensional vector of displacements; $\mathbf{u}(t)$ is an m-dimensional control-force vector; $\mathbf{D}$ is an $n \times m$ matrix representing the locations of the control forces; $\mathbf{F}(t) = [f_1, f_2, \ldots, f_n]^{\mathrm{T}}$ is an n-dimensional external loading vector; and the superscript T denotes vector or matrix transpose.

Let $\mathbf{z}(t) = \mathbf{\Phi}\mathbf{q}(t)$, where $\mathbf{\Phi}$ is a modal matrix and $\mathbf{q}$ is the vector of modal displacement. Then Eq. (1) can be rewritten in the following decoupled form:

$$\ddot{\mathbf{q}}(t) + \mathrm{diag}(2\xi_j\omega_j)\dot{\mathbf{q}}(t) + \mathrm{diag}(\omega_j^2)\mathbf{q}(t) = \mathbf{V}(t) + \mathbf{W}(t), \tag{2}$$

where

$$\mathrm{diag}(2\xi_j\omega_j) = (\mathbf{M}^*)^{-1}\mathbf{C}^*, \quad \mathrm{diag}(\omega_j^2) = (\mathbf{M}^*)^{-1}\mathbf{K}^*, \tag{3a}$$

$$\mathbf{V}(t) = (\mathbf{M}^*)^{-1}\mathbf{\Phi}^{\mathrm{T}}\mathbf{D}\mathbf{u}(t) = \mathbf{L}\mathbf{u}(t), \quad \mathbf{W}(t) = (\mathbf{M}^*)^{-1}\mathbf{\Phi}^{\mathrm{T}}\mathbf{F}(t) = \mathbf{N}\mathbf{F}(t), \tag{3b}$$

$$\mathbf{M}^* = \mathbf{\Phi}^{\mathrm{T}}\mathbf{M}\mathbf{\Phi} = \mathrm{diag}(m_j^*), \quad \mathbf{C}^* = \mathbf{\Phi}^{\mathrm{T}}\mathbf{C}\mathbf{\Phi} = \mathrm{diag}(c_j^*), \tag{3c}$$

$$\mathbf{K}^* = \mathbf{\Phi}^{\mathrm{T}}\mathbf{K}\mathbf{\Phi} = \mathrm{diag}(k_j^*), \quad \mathbf{L} = (\mathbf{M}^*)^{-1}\mathbf{\Phi}^{\mathrm{T}}\mathbf{D}, \tag{3d}$$

$$\mathbf{N} = (\mathbf{M}^*)^{-1}\mathbf{\Phi}^{\mathrm{T}}. \tag{3e}$$

For practical considerations, the design of a structural control system is usually carried out based on the first R modes, referred to as the reduced order system. Then Eq. (2) can be rewritten as

$$\ddot{\mathbf{q}}_c + \mathrm{diag}(2\xi_{jc}\omega_{jc})\dot{\mathbf{q}}_c(t) + \mathrm{diag}(\omega_{jc}^2)\mathbf{q}_c(t) = \mathbf{V}_c(t) + \mathbf{W}_c(t) \quad (j = 1, 2, \ldots, R), \tag{4}$$

where

$$\mathbf{V}_c(t) = \mathbf{L}_c\mathbf{u}(t), \tag{5a}$$

$$\mathbf{W}_c(t) = \mathbf{N}_c\mathbf{F}(t). \tag{5b}$$

In Eq. (4), $\mathbf{q}_c$ is the controlled modal displacement vector of the system, its dimension is, in general, much smaller than that of $\mathbf{q}(t)$. In the modal space, the control vector $\mathbf{V}_c(t)$ is related to the physical control force vector $\mathbf{u}(t)$ by Eq. (5a), and the modal loading vector $\mathbf{W}_c$ is associated with the external loading by Eq. (5b). $\mathbf{L}_c = (\mathbf{L})_{R\times m}$ is an $R \times m$ sub-matrix of $\mathbf{L}$ and $\mathbf{N}_c = (\mathbf{N})_{R\times n}$ is an $R \times n$ sub-matrix of $\mathbf{N}$.

The control force vector in physical space can be simply found by Eq. (5a) as

$$\mathbf{u}(t) = \mathbf{L}^{+}\mathbf{V}_c(t), \tag{6}$$

where $\mathbf{L}^{+}$ is a pseudo-inverse matrix of $\mathbf{L}_c$

$$\mathbf{L}^{+} = (\mathbf{L}_c^{\mathrm{T}}\mathbf{L}_c)^{-1}\mathbf{L}_c^{\mathrm{T}}. \tag{7}$$

Eq. (4) is usually a set of coupled equations since the modal control forces $\mathbf{V}_c(t)$ depend on all the controlled modes. To avoid re-coupling a decoupled control system, the modal control vector $\mathbf{V}_c(t)$ can be designated as

$$\mathbf{V}_c(t) = -\mathbf{G}_1\mathbf{q}_c(t) - \mathbf{G}_2\dot{\mathbf{q}}_c(t), \tag{8}$$

where matrices $\mathbf{G}_1 = \mathrm{diag}(g_{1j})$ and $\mathbf{G}_2 = \mathrm{diag}(g_{2j})$ $(j = 1, 2, \ldots, R)$.

Then, all equations in Eq. (4) are completely independent. The control algorithms based on this design procedure have been referred to as control modal synthesis or, more commonly, the IMSC [10,11].

By means of the classical LQR control law, the feedback gain matrices $\mathbf{G}_1$ and $\mathbf{G}_2$ can be obtained by minimizing a quadratic performance index J if Eq. (4) is expressed as a state-space equation form [12].

3. Effects of control forces on uncontrolled modes

The IMSC algorithm can considerably simplify the structural control design since it shifts the problem from a coupled higher order system to a lower order decoupled system. It is particularly attractive for the cases in which only a few critical modes need to be controlled. However, the response of the controlled system may be underestimated if the effects of the modal control forces on the uncontrolled modes are not considered in the design. In some cases, the modal control forces may significantly increase the contributions of uncontrolled modes to the vibration of the system, especially for a flexible structure, in which the contributions of its higher modes cannot be ignored. This statement can be verified as follows. The equations for uncontrolled modes are

$$\ddot{\mathbf{q}}_r + \mathrm{diag}(2\xi_{jr}\omega_{jr})\dot{\mathbf{q}}_r(t) + \mathrm{diag}(\omega_{jr}^2)\mathbf{q}_r(t) = \mathbf{V}_r(t) + \mathbf{W}_r(t) \quad (j = R+1, R+2, \ldots, n), \tag{9}$$

where $\mathbf{q}_r$ is uncontrolled mode co-ordinate, and

$$\mathbf{V}_r(t) = \mathbf{L}_r\mathbf{u}(t), \quad \mathbf{W}_r(t) = \mathbf{N}_r\mathbf{F}(t). \tag{10}$$

Using Eqs. (6) and (8), one obtains

$$\mathbf{V}_r(t) = \mathbf{L}_r\mathbf{L}^+\mathbf{V}_c(t) = -\mathbf{L}_r\mathbf{L}^+\mathbf{G}\mathbf{Q}(t), \tag{11}$$

where $\mathbf{L}_r = (\mathbf{L})_{(n-R)\times m}$ is a $(n-R)\times m$ sub-matrix of $\mathbf{L}$ and

$$\mathbf{G} = [\mathbf{G}_1, \mathbf{G}_2], \quad \mathbf{Q}(t) = [\mathbf{q}_c(t), \dot{\mathbf{q}}_c(t)]^{\mathrm{T}}. \tag{12}$$

Eq. (9) shows that the modal control forces play the same role as the external excitation to the uncontrolled modes, which may amplify the contributions of the uncontrolled modes to the system's vibration. Meanwhile, the response of the system may be underestimated if such contributions are not considered in response analysis.

By investigating the responses of the uncontrolled modes induced by control forces and external excitations, the effects of the modal control forces on the uncontrolled modes can be easily assessed. For simplicity, suppose only the first mode is controlled and the number of control forces is equal to the number of the d.o.f., i.e., $R = 1$ and $m = n$. Thus, $\mathbf{D}$ is a unit matrix.

Rewrite Eq. (4) as

$$\dot{\mathbf{Y}} = \mathbf{A}\mathbf{Y} + \mathbf{B}_1 V_{c1}(t) + \mathbf{D}_1 W_{c1}(t), \tag{13}$$

where $\mathbf{Y} = (q_1, \dot{q}_1)^{\mathrm{T}}$ and

$$\mathbf{A} = \begin{bmatrix} 0 & 1 \\ -\omega_1^2 & -2\xi_1\omega_1 \end{bmatrix}, \quad \mathbf{B}_1 = \mathbf{D}_1 = [0 \quad 1]^{\mathrm{T}}, \tag{14}$$

the control forces $\mathbf{u}(t) = [u_1, u_2, \ldots, u_n]^{\mathrm{T}}$ are related to V_{c1} by $V_{c1} = (\sum_{j=1}^{n} \varphi_{j,1}u_j)/m_1^*$, the external excitation vector $\mathbf{F}(t) = [f_1, f_2, \ldots, f_n]^{\mathrm{T}}$ has the relationship with W_{c1} by $E_{c1} = (\sum_{j=1}^{n} \varphi_{j,1}f_j)/m_1^*$; here $\varphi_{j,1}$ is the jth element of the fundamental mode; ξ_1 and ω_1 are the critical damping ratio and the circular natural frequency of the first mode, respectively.

The modal control force V_{c1} can be determined by the classical LQR control law and the quadratic performance index J is

$$J = \int_0^{t_f} (\mathbf{Y}^{\mathrm{T}}\mathbf{Q}\mathbf{Y} + RV_{c1}^2)\,\mathrm{d}t, \tag{15}$$

where $\mathbf{Q}$ is a positive definite or a semi-positive definite weight matrix, and $R > 0$. Minimizing J gives the modal control force V_{c1} as

$$V_{c1} = -\frac{1}{R}\mathbf{B}_1^{\mathrm{T}}\mathbf{P}\mathbf{Y}. \tag{16}$$

The matrix $\mathbf{P}$ satisfies the following Riccati matrix equation if the control time t_f is long enough:

$$\mathbf{P}\mathbf{A} + \mathbf{A}^{\mathrm{T}}\mathbf{P} - \frac{1}{R}\mathbf{P}\mathbf{B}_1\mathbf{B}_1^{\mathrm{T}}\mathbf{P} + \mathbf{Q} = \mathbf{0}. \tag{17}$$

Let weight matrix $\mathbf{Q}$ be diag(Q_j), and rewrite $\mathbf{P}$ as

$$\mathbf{P} = \begin{bmatrix} p_1 & p_2 \\ p_2 & p_3 \end{bmatrix},$$

the modal control force V_{c1} is given by

$$V_{c1}(t) = -\frac{p_2}{R} q_1(t) - \frac{p_3}{R} \dot{q}_1(t), \tag{18}$$

and the solutions of Eq. (17) are

$$p_1 = 2\xi_1\omega_1 p_2 + \omega_1^2 p_3 + \frac{p_2 p_3}{R}, \tag{19a}$$

$$p_2 = \omega_1^2 R\left(\sqrt{1 + \frac{Q_1}{R\omega_1^4}} - 1\right), \tag{19b}$$

$$p_3 = 2\xi_1\omega_1 R\left(\sqrt{1 + \frac{2p_2 + Q_2}{(2\xi_1\omega_1)^2 R}} - 1\right). \tag{19c}$$

Then the equation of the controlled mode (first mode), and the modal control force V_{c1} are

$$\ddot{q}_1(t) + 2\xi_1\omega_1(1+\beta)\dot{q}_1(t) + \omega_1^2(1+\gamma)q_1(t) = W_{c1}(t), \tag{20}$$

$$V_{c1}(t) = -\gamma\omega_1^2 q_1(t) - 2\beta\xi_1\omega_1\dot{q}_1(t), \tag{21}$$

where

$$\beta = \sqrt{1 + \frac{2p_2 + Q_2}{(2\xi_1\omega_1)^2 R}} - 1 > 0, \quad \gamma = \sqrt{1 + \frac{Q_1}{\omega_1^4 R}} - 1 > 0. \tag{22}$$

It can be seen, from Eq. (20), that the modal control force V_{c1} provides the active modal damping and stiffness to the first mode.

Suppose that the power spectral density (PSD) matrix of excitation is $\mathbf{S}_F(\omega)$, the PSD of the modal excitation of the fundamental mode is

$$S_{W_{c1}}(\omega) = \left(\frac{1}{m_1^*}\right)^2 \varphi_1^T \mathbf{S}_F(\omega)\varphi_1, \tag{23}$$

where φ_1 is the first mode shape vector.

The variance and the PSD of the modal control force are

$$\sigma_{V_{c1}}^2 = \gamma^2\omega_1^4\sigma_{q_1}^2 + 4\beta^2\xi_1^2\omega_1^2\sigma_{\dot{q}_1}^2, \tag{24a}$$

$$S_{V_{c1}}(\omega) = (\gamma^2\omega_1^4 + 4\beta^2\xi_1^2\omega_1^2\omega^2)|H_1(\omega)|^2 S_{W_{c1}}(\omega), \tag{24b}$$

where $|H_1(\omega)|^2 = 1/[(\omega^2 - \omega_1^2(1+\gamma)^2)^2 + (2\xi_1\omega_1\omega(1+\beta))^2]$; $\sigma_{q_1}^2$ and $\sigma_{\dot{q}_1}^2$ are the variances of the modal displacement and the modal velocity of the fundamental mode, respectively.

Substituting Eq. (11) into Eq. (9) yields

$$\ddot{q}_i(t) + 2\xi_i\omega_i\dot{q}_i(t) + \omega_i^2 q_i(t) = -\lambda_i V_{c1}(t) + w_i(t) \quad (i = 2, 3, \ldots, n), \tag{25}$$

where

$$\lambda_i = \frac{m_1^*}{m_i^*}\,\varphi_i^{\mathrm{T}}(\varphi_1\varphi_1^{\mathrm{T}})^{-1}\varphi_1, \tag{26a}$$

$$w_i(t) = \frac{1}{m_i^*}\sum_{j=1}^{n}\varphi_{j,i}f_j, \tag{26b}$$

$$S_{w_i}(\omega) = \frac{1}{(m_i^*)^2}\,\varphi_i^{\mathrm{T}}\mathbf{S}_F(\omega)\varphi_i \quad (i = 2, 3, \ldots, n). \tag{26c}$$

The PSD of the response of the ith ($i = 2, 3, \ldots, n$) mode is

$$S_{q_i}(\omega) = |H_i(\omega)|^2[\lambda_i^2 S_{V_{c1}}(\omega) + S_{e_{ri}}(\omega)], \tag{27}$$

where $|H_i(\omega)|^2 = 1/[(\omega^2 - \omega_i^2)^2 + (2\xi_i\omega_i\omega)^2]$.

It can be seen from Eq. (27) that the modal control force may intensify the vibration of the uncontrolled modes. If the external excitation is a Gaussian white noise with spectral intensity S_0, Eqs. (24b) and (26c) can be simplified as follows.

The PSD of the modal control force is

$$S_{V_{c1}}(\omega) = (\gamma^2\omega_1^4 + 4\beta^2\xi_1^2\omega_1^2\omega^2)|H_1(\omega)|^2\mu S_0. \tag{28a}$$

The PSD of the modal excitation is

$$S_{w_i}(\omega) = \frac{\varphi_i^{\mathrm{T}}\varphi_i}{(m_i^*)^2}\,S_0 \quad (i = 2, 3, \ldots, n). \tag{28b}$$

Therefore, the variances of responses of the ith ($i = 2, 3, \ldots, n$) mode corresponding to the modal control forces and external excitations are:

$$\sigma_{q_i}^2|_{V_{c1}} = \int_{-\infty}^{\infty} |H_1(\omega)|^2|H_i(\omega)|^2(\gamma^2\omega_1^4 + 4\xi_1\omega_1^2\omega^2)\lambda_i^2\mu S_0, \tag{29a}$$

$$\sigma_{\dot{q}_i}^2|_{V_{c1}} = \int_{-\infty}^{\infty} \omega^2|H_1(\omega)|^2|H_i(\omega)|^2(\gamma^2\omega_1^4 + 4\xi_1\omega_1^2\omega^2)\lambda_i^2\mu S_0, \tag{29b}$$

$$\sigma_{\ddot{q}_i}^2|_{V_{c1}} = \int_{-\infty}^{\infty} \omega^4|H_1(\omega)|^2|H_i(\omega)|^2(\gamma^2\omega_1^4 + 4\xi_1\omega_1^2\omega^2)\lambda_i^2\mu S_0, \tag{29c}$$

$$\sigma_{q_i}^2|_{e_{ri}} = \frac{\pi\mu_i S_0}{2\xi_i\omega_i^3}, \tag{29d}$$

$$\sigma_{\dot{q}_i}^2|_{e_{ri}} = \frac{\pi\mu_i S_0}{2\xi_i\omega_i}, \tag{29e}$$

$$\sigma_{\ddot{q}_i}^2|_{e_{ri}} = \frac{\pi\omega_i\mu_i S_0}{2\xi_i}, \tag{29f}$$

where

$$\mu_i = \frac{\sum_{j=1}^{n} \varphi_{j,i}^2}{(m_i^*)^2}.$$

The effects of the modal control forces on the uncontrolled modes can be easily assessed by Eqs. (29). The quantitative descriptions of these effects are given by the following numerical example, in which the performance of a six-story building subjected to the white noise base excitation is examined.

4. Numerical example 1

A six-story building is modelled as a m.d.o.f. system shown in Fig. 1. The lumped mass at each floor is, $m_i = m = 3.456 \times 10^3$ kg $(i = 1, 2, \ldots, 6)$ and inter-story stiffness is $k_i = k = 3.405 \times 10^5$ kN/m. The values of the critical damping ratio are $\xi_1 = 1\%$, $\xi_2 = 1.5\%$, $\xi_3 = 2\%$, $\xi_4 = 2.5\%$, $\xi_5 = 3\%$, $\xi_6 = 3.5\%$, and the values of circular natural frequencies, modal mass and modal stiffness are given in Appendix A.

The base excitation is modeled as a band-limited Gaussian white noise with intensity $S_0 = 0.0159$ m^2/s^3 and bandwidth=10 Hz. The following algorithm proposed by Shinozuka [13] is used to generate the time histories of the base excitation.

$$f(t) = \sum_{k=1}^{N} a_k \cos(\omega_k t + \phi_k), \tag{30}$$

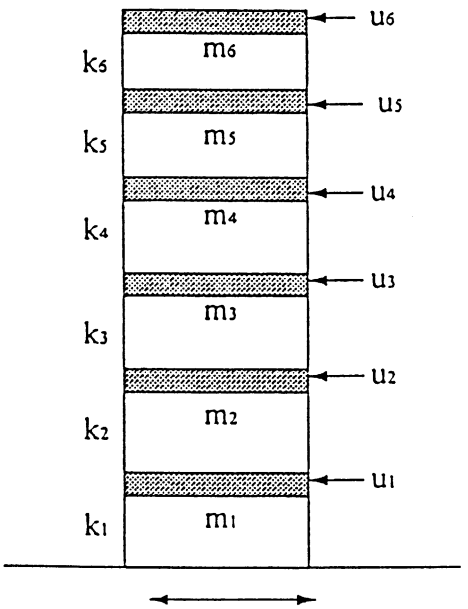

Fig. 1. The analytical model of the six-story building.

where N is the number of intervals along the frequency axis and

$$\Delta\omega = (\omega_u - \omega_l)/N,$$

$$\omega_k = \omega_l + (k_i + 1/2)\Delta\omega \quad (k = 1, 2, \ldots, N),$$

ϕ_k is independent random phase uniformly distributed between 0 and 2π; a_k is independent Gaussian random variable with $(0, \sigma_k^2)$, in which $\sigma_k^2 = 4S_0\Delta\omega$ $(k = 1, 2, \ldots, N)$.

Fig. 2 shows the simulated time histories of the base excitation based on the above algorithm.

Assume that

$$\mathbf{Q} = \begin{bmatrix} 57.2 & 0 \\ 0 & 1 \end{bmatrix}, \quad R = 2.0,$$

and the control design is carried out based on the first mode, Eq. (22) gives $\beta = 5.6881$, $\gamma = 0.0044$, and the modal control force V_{c1} is

$$V_{c1} = -0.2517q_1 - 0.8606\dot{q}_1.$$

The variances of responses of the second mode including and not including the effects of the modal control forces are calculated, respectively, as follows.

$$\sigma_{q_2}^2|_{w_{r1}} = 2.8227 \times 10^{-6}, \quad \sigma_{q_2}^2|_{w_{r1}+V_{c1}} = 3.3262 \times 10^{-6},$$

$$\sigma_{\dot{q}_2}^2|_{w_{r1}} = 9.8334 \times 10^{-4}, \quad \sigma_{\dot{q}_2}^2|_{w_{r1}+V_{c1}} = 0.0011,$$

$$\sigma_{\ddot{q}_2}^2|_{w_{r1}} = 0.5448, \quad \sigma_{\ddot{q}_2}^2|_{w_{r1}+V_{c1}} = 0.5687.$$

It can be seen from the above results that, due to the effects of the modal control force, the variances of modal displacement, modal velocity and modal acceleration increase 17.84%, 11.86% and 4.22%, respectively. This suggests that the effects of the modal control force on the uncontrolled modes should be examined carefully when the control design is carried out based on the IMSC algorithm, especially for a flexible structure in which the vibration is dominated by several modes.

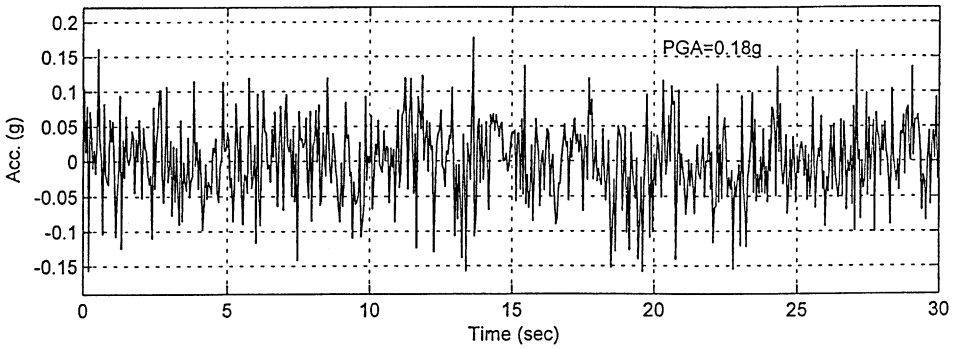

Fig. 2. Simulated acceleration of ground motion.

5. Modified independent modal space control algorithm

As discussed above, the responses of the uncontrolled modes can be amplified by the control forces using the IMSC control method. In this case, the contributions of the uncontrolled modes may be significant and the structural response may be underestimated if such contributions are ignored in the response analysis. It will be shown that the control algorithm, modified independent modal space control (MIMSC), will eliminate the effects of the modal control forces on the uncontrolled modes, so that the control system will be more effective than that based on the IMSC.

Rewrite Eq. (2) as follows:

$$\mathbf{M}^*\ddot{\mathbf{q}}(t) + \mathbf{C}^*\dot{\mathbf{q}}(t) + \mathbf{K}^*\mathbf{q}(t) = \mathbf{\Phi}^{\mathrm{T}}\mathbf{D}u(t) + \mathbf{\Phi}^{\mathrm{T}}\mathbf{F}(t) \tag{31}$$

or

$$\mathbf{M}^*\ddot{\mathbf{q}}(t) + \mathbf{C}^*\dot{\mathbf{q}}(t) + \mathbf{K}^*\mathbf{q}(t) = \mathbf{H}u(t) + \mathbf{E}(t). \tag{31a}$$

Suppose the number of the controlled modes is R, matrices H and E can be rewritten as partition form:

$$\mathbf{H} = \mathbf{\Phi}^{\mathrm{T}}\mathbf{D} = \begin{bmatrix} (\mathbf{H}_c)_{R\times m} \\ (\mathbf{H}_r)_{(n-R)\times m} \end{bmatrix}, \quad \mathbf{E} = \mathbf{\Phi}^{\mathrm{T}}\mathbf{F}(t) = \begin{bmatrix} (\mathbf{E}_c)_{R\times 1} \\ (\mathbf{E}_r)_{(n-R)\times 1} \end{bmatrix}.$$

Therefore, the equations for the controlled modes and uncontrolled modes are:

For the controlled modes:

$$\mathbf{M}_c^*\ddot{\mathbf{q}}_c(t) + \mathbf{C}_c^*\dot{\mathbf{q}}(t) + \mathbf{K}_c^*\mathbf{q}_c(t) = \mathbf{H}_c\mathbf{u}(t) + \mathbf{E}_c(t). \tag{32a}$$

For the uncontrolled modes:

$$\mathbf{M}_r^*\ddot{\mathbf{q}}_r(t) + \mathbf{C}_r^*\dot{\mathbf{q}}(t) + \mathbf{K}_r^*\mathbf{q}_r(t) = \mathbf{H}_r\mathbf{u}(t) + \mathbf{E}_r(t), \tag{32b}$$

where

$$\mathbf{H}_c = (\mathbf{\Phi}^{\mathrm{T}}\mathbf{D})_{R\times m}, \quad \mathbf{H}_r = (\mathbf{\Phi}^{\mathrm{T}}\mathbf{D})_{(n-R)\times m}, \tag{33a}$$

$$\mathbf{M}_c^* = (\mathbf{M}^*)_{R\times R}, \quad \mathbf{M}_r^* = (\mathbf{M}^*)_{(n-R)\times(n-R)}, \tag{33b}$$

$$\mathbf{C}_c^* = (\mathbf{M}^*)_{(R\times R)}, \quad \mathbf{C}_r^* = (\mathbf{C}^*)_{(n-R)\times(n-R)}, \tag{33c}$$

$$\mathbf{K}_c^* = (\mathbf{K}^*)_{(R\times R)}, \quad \mathbf{K}_r^* = (\mathbf{K}^*)_{(n-R)\times(n-R)}, \tag{33d}$$

in which $(\mathbf{A})_{s\times t}$ is a $s \times t$ sub-matrix of matrix $\mathbf{A}$.

Let

$$\mathbf{u}(t) = -\mathbf{G}_1\mathbf{q}_c - \mathbf{G}_2\dot{\mathbf{q}}_c. \tag{34}$$

Eq. (32) are expressed as

For the controlled modes:

$$\mathbf{M}_c^*\ddot{\mathbf{q}}_c(t) + (\mathbf{C}_c^* + \mathbf{H}_c\mathbf{G}_2)\dot{\mathbf{q}}_c(t) + (\mathbf{K}_c^* + \mathbf{H}_c\mathbf{G}_1)\mathbf{q}_c(t) = \mathbf{E}_c(t). \tag{35a}$$

For the uncontrolled modes:

$$\mathbf{M}_r^*\ddot{\mathbf{q}}_r(t) + \mathbf{C}_r^*\dot{\mathbf{q}}_r(t) + \mathbf{K}_r^*\mathbf{q}_r(t) = -\mathbf{H}_r[\mathbf{G}_1\mathbf{q}_c(t) + \mathbf{G}_2\dot{\mathbf{q}}_c(t)] + \mathbf{E}_r(t). \tag{35b}$$

Consider the following conditions:

1. Both $\mathbf{H}_c\mathbf{G}_1$ and $\mathbf{H}_c\mathbf{G}_2$ are diagonal matrices.
2. $\mathbf{H}_r\mathbf{G}_1 = \mathbf{H}_r\mathbf{G}_2 = \mathbf{0}$.

It is obvious that Eq. (35a) is a set of decoupled equations and no effects of the control forces on the uncontrolled modes exist in Eq. (35b) if the above two conditions are satisfied.

Rewrite conditions 1 and 2 in the following forms:

$$\mathbf{H}\mathbf{G}_1 = \begin{bmatrix} s_1 & & \\ & \ddots & \\ & & s_R \\ 0 & \cdots & 0 \\ \cdots & \cdots & \cdots \\ 0 & \cdots & 0 \end{bmatrix} = \begin{bmatrix} \mathbf{s} \\ \mathbf{0} \end{bmatrix}_{n\times R}, \qquad \mathbf{H}\mathbf{G}_2 = \begin{bmatrix} d_1 & & \\ & \ddots & \\ & & d_R \\ 0 & \cdots & 0 \\ \cdots & \cdots & \cdots \\ 0 & \cdots & 0 \end{bmatrix} = \begin{bmatrix} \mathbf{d} \\ \mathbf{0} \end{bmatrix}_{n\times R}, \tag{36}$$

where

$$\mathbf{H} = \begin{bmatrix} \mathbf{H}_c \\ \mathbf{H}_r \end{bmatrix}.$$

Eq. (36) shows that the feedback gain matrices can be obtained if the diagonal matrices $\mathbf{s}$ and $\mathbf{d}$ are determined based on the same algorithm.

Suppose that the number of control forces m is equal to n, i.e., equal to the number of d.o.f. of the system, then $\mathbf{H} = \mathbf{\Phi}^{\mathrm{T}}$ (note that the condition $m \geqslant R$ must be satisfied in this algorithm. Refer to Appendix B). Without loss of generality, it is assumed that $\mathbf{G}_1 = \mathbf{M}\mathbf{\Phi}\mathbf{F}_1$ and $\mathbf{G}_2 = \mathbf{M}\mathbf{\Phi}\mathbf{F}_2$. Left multiplying $\mathbf{\Phi}^{\mathrm{T}}$ to $\mathbf{G}_1$ and $\mathbf{G}_2$ and using the orthogonal property of the mode shapes, yields

$$\mathbf{F}_1 = [\mathbf{M}^*]^{-1}\begin{bmatrix} \mathbf{s} \\ \mathbf{0} \end{bmatrix}, \quad \mathbf{F}_2 = [\mathbf{M}^*]^{-1}\begin{bmatrix} \mathbf{d} \\ \mathbf{0} \end{bmatrix}. \tag{37}$$

Then

$$\mathbf{G}_1 = \mathbf{M}\mathbf{\Phi}_c[\mathbf{M}_c^*]^{-1}\mathbf{s}, \quad \mathbf{G}_2 = \mathbf{M}\mathbf{\Phi}_c[\mathbf{M}_c^*]^{-1}\mathbf{d}, \tag{38}$$

where $\mathbf{\Phi}_c = (\mathbf{\Phi})_{n\times R}$, i.e., $\mathbf{\Phi}_c$ is a matrix constituted by the first R mode shapes.

Condition 2 is automatically satisfied, since

$$\mathbf{H}_r\mathbf{G}_1 = \mathbf{\Phi}_r^{\mathrm{T}}\mathbf{M}\mathbf{\Phi}_c[\mathbf{M}_c^*]^{-1}\mathbf{s} = \mathbf{0}, \quad \mathbf{H}_r\mathbf{G}_2 = \mathbf{\Phi}_r^{\mathrm{T}}\mathbf{M}\mathbf{\Phi}_c[\mathbf{M}_c^*]^{-1}\mathbf{d} = \mathbf{0}. \tag{39}$$

The matrices $\mathbf{G}_1 = (g_{ij})_{n\times R}$ and $\mathbf{G}_2 = (\bar{g}_{ij})_{n\times R}$ can be expressed as

$$g_{ij} = \frac{m_i\varphi_{i,j}s_j}{m_j^*}, \qquad \bar{g}_{ij} = \frac{m_i\varphi_{i,j}d_j}{m_j^*} \quad (i = 1, 2, \ldots, n;\ j = 1, 2, \ldots, R). \tag{40}$$

It is therefore, quite clear that the feedback gain matrices can be obtained if the diagonal matrices **s** and **d** are known. The LQR control law is used to determine matrices **s** and **d** as follows.

Rewrite Eq. (32a) as a state-space equation

$$\dot{\mathbf{Y}} = \mathbf{A}\mathbf{Y} + \mathbf{D}\mathbf{E}_c(t) + \mathbf{B}\mathbf{u}(t), \tag{41}$$

where $\mathbf{Y} = [\mathbf{q}_c, \dot{\mathbf{q}}_c]^{\mathrm{T}}$ and

$$\mathbf{A} = \begin{bmatrix} \mathbf{0} & \mathbf{I} \\ -\mathrm{diag}(\omega_j^2) & -\mathrm{diag}(2\xi_j\omega_j) \end{bmatrix}, \quad \mathbf{D} = \begin{bmatrix} \mathbf{0} \\ [\mathbf{M}_c^*]^{-1} \end{bmatrix}, \quad \mathbf{B} = \begin{bmatrix} \mathbf{0} \\ [\mathbf{M}_c^*]^{-1}\mathbf{\Phi}_c^{\mathrm{T}} \end{bmatrix}.$$

The quadratic performance index J is

$$J = \int_0^{t_f} (\mathbf{Y}^{\mathrm{T}}\mathbf{Q}\mathbf{Y} + \mathbf{u}^{\mathrm{T}}\mathbf{R}\mathbf{u})\,\mathrm{d}t. \tag{42}$$

The weight matrix $\mathbf{Q}$ is chosen as the form

$$\mathbf{Q} = \begin{bmatrix} \mathbf{Q}_1 & \mathbf{0} \\ \mathbf{0} & \mathbf{Q}_2 \end{bmatrix},$$

in which sub-matrices $\mathbf{Q}_1$ and $\mathbf{Q}_2$ are diagonal matrices. The control force vector $\mathbf{u}(t)$ is given by

$$\mathbf{u}(t) = -\mathbf{R}^{-1}\mathbf{B}^{\mathrm{T}}\mathbf{P}\mathbf{Y}. \tag{43}$$

$\mathbf{P}$ satisfies the following Riccati matrix equation:

$$\mathbf{P}\mathbf{A} + \mathbf{A}^{\mathrm{T}}\mathbf{P} - \mathbf{P}\mathbf{B}\mathbf{R}^{-1}\mathbf{B}^{\mathrm{T}}\mathbf{P} + \mathbf{Q} = \mathbf{0}. \tag{44}$$

Rewrite $\mathbf{P}$ as partition form

$$\mathbf{P} = \begin{bmatrix} \mathbf{P}_{11} & \mathbf{P}_{21} \\ \mathbf{P}_{21} & \mathbf{P}_{22} \end{bmatrix},$$

then the sub-matrices $\mathbf{P}_{21}$ and $\mathbf{P}_{22}$ satisfy the following equations:

$$\mathbf{P}_{21}[\mathbf{M}_c^*]^{-1}\mathbf{K}_c^* + [\mathbf{M}_c^*]^{-1}\mathbf{K}_c^*\mathbf{P}_{21} + \mathbf{P}_{21}[\mathbf{M}_c^*]^{-1}\mathbf{\Phi}_c^{\mathrm{T}}\mathbf{R}^{-1}\mathbf{\Phi}_c[\mathbf{M}_c^*]^{-1}\mathbf{P}_{21} - \mathbf{Q}_1 = \mathbf{0}, \tag{45a}$$

$$\mathbf{P}_{22}[\mathbf{M}_c^*]^{-1}\mathbf{C}_c^* + [\mathbf{M}_c^*]^{-1}\mathbf{C}_c^*\mathbf{P}_{22} + \mathbf{P}_{22}[\mathbf{M}_c^*]^{-1}\mathbf{\Phi}_c^{\mathrm{T}}\mathbf{R}^{-1}\mathbf{\Phi}_c[\mathbf{M}_c^*]^{-1}\mathbf{P}_{22} - 2\mathbf{P}_{21} - \mathbf{Q}_2 = \mathbf{0}. \tag{45b}$$

The control force vector is given by

$$\mathbf{u}(t) = -\mathbf{R}^{-1}\mathbf{\Phi}_c[\mathbf{M}_c^*]^{-1}\mathbf{P}_{21}\mathbf{q}_c - \mathbf{R}^{-1}\mathbf{\Phi}_c[\mathbf{M}_c^*]^{-1}\mathbf{P}_{22}\dot{\mathbf{q}}_c. \tag{46}$$

By the comparison of Eq. (38) with Eq. (46), one has

$$\mathbf{M}\mathbf{\Phi}_c[\mathbf{M}_c^*]^{-1}\mathbf{s} = \mathbf{R}^{-1}\mathbf{\Phi}_c[\mathbf{M}_c^*]^{-1}\mathbf{P}_{21}, \tag{47a}$$

$$\mathbf{M}\mathbf{\Phi}_c[\mathbf{M}_c^*]^{-1}\mathbf{d} = \mathbf{R}^{-1}\mathbf{\Phi}_c[\mathbf{M}_c^*]^{-1}\mathbf{P}_{22}. \tag{47b}$$

If the weight matrix $\mathbf{R}$ is chosen as

$$\mathbf{R}^{-1} = \frac{1}{R_1}\mathbf{M}, \tag{48}$$

and substituting Eq. (48) into Eq. (47), one has

$$\mathbf{P}_{21} = R_1\mathbf{s}, \quad \mathbf{P}_{22} = R_1\mathbf{d}, \tag{49}$$

where R_1 is a constant that can be selected according to the control conditions.

Therefore, the solutions of Eq. (45) are found as

$$s_j = k_j^*\left(\sqrt{1+\frac{Q_{1j}m_j^*}{R_1(k_j^*)^2}}-1\right), \tag{50a}$$

$$d_j = c_j^*\left(\sqrt{1+\frac{L_j m_j^*}{R_1(c_j^*)^2}}-1\right), \tag{50b}$$

where

$$L_j = \frac{m_j^* Q_{1j}}{2k_j^* + s_j} + Q_{2j} \quad (j = 1, 2, \ldots, R). \tag{51}$$

By substituting Eq. (50) into Eq. (40), the feedback gain matrices $\mathbf{G}_1$ and $\mathbf{G}_2$ can be obtained.

6. Numerical example 2

The structural model examined in the numerical example 1 is used herein to illustrate the effectiveness of the proposed algorithm, and to study the effects of the control forces on the uncontrolled modes. The same assumptions are made as those given in the numerical example 1, i.e., $m = n$, $R = 1$. The weight matrices $\mathbf{Q}$ and $\mathbf{R}$ are chosen as

$$\mathbf{Q} = \begin{bmatrix} 10^5 & 0 \\ 0 & 10^5 \end{bmatrix}, \quad \mathbf{R} = 0.1\mathbf{M}^{-1}. \tag{52}$$

Substituting $Q_1 = Q_2 = 10^5$ and $R_1 = 0.1$ into Eq. (50), one obtains $s_1 = 8.725 \times 10^3$ and $d_1 = 5.396 \times 10^5$. Then, the feedback gain matrices $\mathbf{G}_1$ $\mathbf{G}_2$ can be determined by Eq. (40) as $\mathbf{G}_1 = [1158, 2249, 3209, 3983, 4525, 4805]^{\mathrm{T}}$ and $\mathbf{G}_2 = [71610, 13912, 19848, 24634, 27991, 29717]^{\mathrm{T}}$.

Table 1 lists the maximum responses of the top floor. It can be seen from Table 1 that the displacement, velocity and acceleration responses of the top floor are reduced by 62.2%, 63.6% and 51%, respectively, when the structure is controlled based on the proposed algorithm. Figs. 3, 4 and 5 show the comparison of the responses corresponding to the controlled and uncontrolled structure. These figures show that the responses of the top floor have been significantly reduced.

In order to investigate the effects of the control forces on the uncontrolled modes, the IMSC algorithm is also used to control the same structure. Figs. 6, 7 and 8 show the structural

Table 1
Responses of the top floor and the control force

	Max. disp (cm)	Max. vel. (cm/s)	Max. acc. (cm/s^2)	r.m.s. disp (cm)	r.m.s. vel. (cm/s)	r.m.s. acc. (cm/s^2)
Uncontrolled	8.88	67.60	613	5.20	38.54	314
Controlled	3.36	24.62	300	1.97	14.28	161
Maximum control force (absolute values)						
Contr. no	$u1$	$u2$	$u3$	$u4$	$u5$	$u6$
Contr. force (KN)	34.12	66.28	94.57	117.74	133.36	141.59

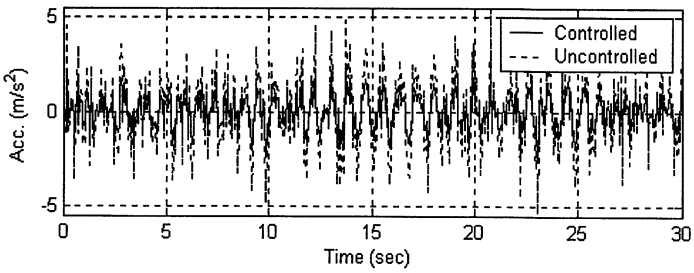

Fig. 3. Acceleration response of the top floor.

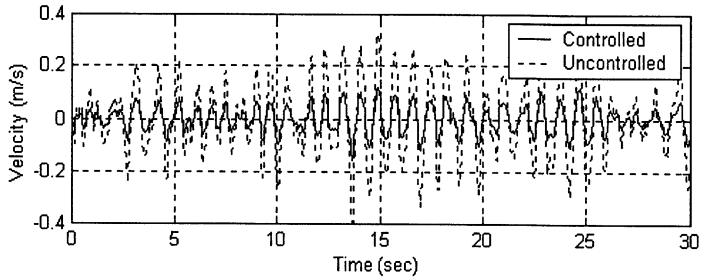

Fig. 4. Velocity response of the top floor.

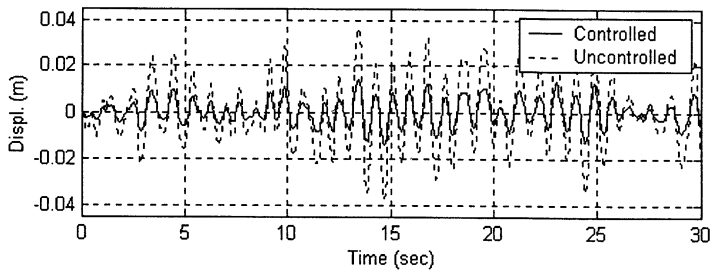

Fig. 5. Displacement response of the top floor.

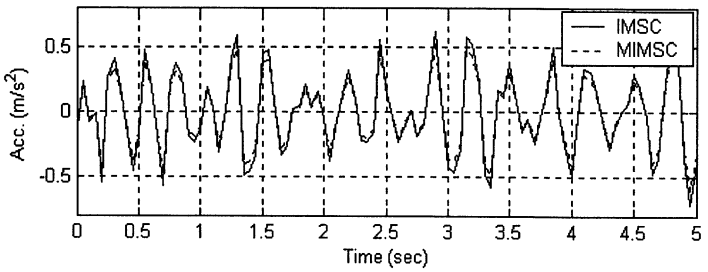

Fig. 6. The contributions of the higher uncontrolled modes to acceleration response.

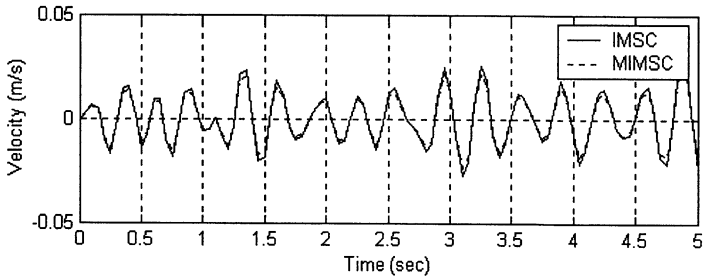

Fig. 7. The contributions of the higher uncontrolled modes to velocity response.

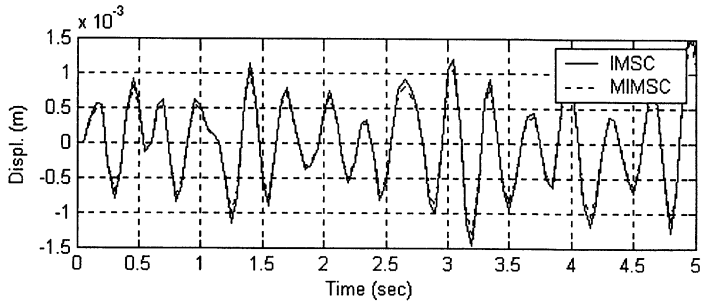

Fig. 8. The contributions of the higher uncontrolled modes to displacement response.

responses contributed by the uncontrolled modes. From these figures, it can be seen that, for the IMSC algorithm, the control forces amplifies the contributions of the higher uncontrolled modes to the responses, and the MIMSC algorithm does not make any contribution to the responses of the higher uncontrolled modes. The acceleration, velocity and displacement responses are increased by 16.3%, 13.2%, and 12.1%, respectively, comparing with those of the MIMSC algorithm. Obviously, for a structure with higher participating coefficients of higher modes, the excitations of the modal control forces to the uncontrolled modes should be examined carefully when the IMSC is used as control algorithm. For clarity, responses with only 5 s duration are shown in Figs. 6–8.

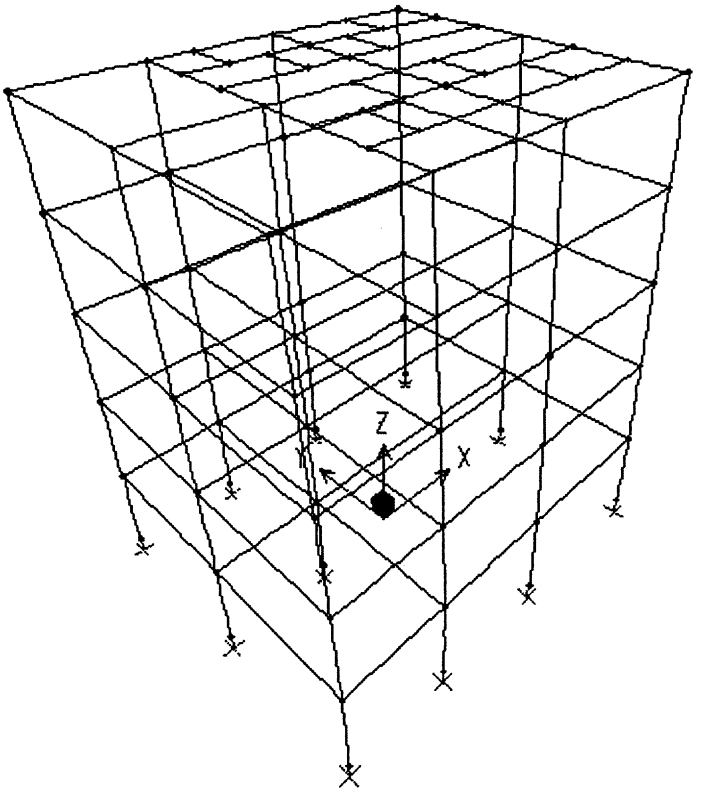

Fig. 9. 3-D finite element model of the building.

7. Active control design of the UCLA Math-Science building

This example addresses the application of the proposed control algorithm in the active control design of the University of California, Los Angeles (UCLA) Math-Science Addition. The building located on UCLA campus is a seven-story moment resisting steel frame building which is separated by 15 cm seismic joint from its adjacent buildings in the north–south (N–S) directions. At lower level of the building there is a very rigid nuclear reactor structure made of reinforced concrete, which makes the building be visualized as a five-story structure. Hart and Fang [14] designed the passive control system for this building using ENIDINE viscous damper devices and gave a detailed introduction on this building.

The objective of installing an active control system is to reduce the roof displacement of this building and to avoid impact with its adjacent buildings in the N–S direction. Finite element method is used to establish the analytic model of the building in the N–S direction in order to perform the active control design. A three-dimensional finite element model of this building is developed using SAP2000 computer program as shown in Fig. 9. The natural periods (s) of the building in the north direction are determined by modal analysis, which are $T_1 = 0.6791$, $T_2 = 0.2217$, $T_3 = 0.1285$, $T_4 = 0.0922$, $T_5 = 0.0905$. Assuming unit forces are applied to each level in the N–S direction and by performing static analysis, the stiffness parameters (10^5 kN/m) in this

direction are obtained, and the stiffness matrix is given as follows:

$$\mathbf{K} = \begin{bmatrix} 4.7875 & -2.4569 & 0.4229 & -0.0497 & -0.0173 \\ -2.4569 & 3.9408 & -2.2843 & 0.3952 & -0.0267 \\ 0.4229 & -2.2843 & 3.7947 & -2.2291 & 0.3424 \\ -0.0497 & 0.3952 & -2.2291 & 3.5582 & -1.6837 \\ -0.0173 & -0.0267 & 0.3424 & -1.6837 & 1.3486 \end{bmatrix}. \quad (53)$$

Lumping all masses to each level obtains the values of lumped mass (10^5 kg) from the roof to the lower floors are, $m_5 = 0.0712$, $m_4 = 0.0870$, $m_3 = 0.148$, $m_2 = 0.2198$, $m_1 = 0.6828$. Based on these stiffness and mass parameters, the natural periods in the N–S direction are re-determined as $T_1 = 0.6828$, $T_2 = 0.2198$, $T_3 = 0.1248$, $T_4 = 0.0870$, $T_5 = 0.0712$. Comparing these values with those given by the finite element analysis shows that the analytic model with the stiffness matrix [Eq. (53)] and the lumped mass captures main properties of the building in the N–S direction.

Evaluation of damping in a structural system poses a difficult problem in structural dynamics, since damping of a structure is not simply related to any single vibration phenomenon [15]. According to Li et al. [16], the critical damping ratio of the first mode is reasonably assumed to be 1–3% for a steel structure. In order to investigate the damping effects on the structural control design based on the proposed algorithm, the damping ratio of the first mode is assumed as $\xi_1 = 1\%$ and 2%, respectively, for this building. Based on an assumption of Rayleigh damping, the damping matrix can be established. Fig. 10 plots the damping ratios of each mode corresponding to the assumption of $\xi_1 = 1\%$, 2% and 5% of the damping ratio of the first mode.

The earthquake record measured at Rinaldi during the Northridge Earthquake in 1994 is adopted as the base excitation for the response analysis of the uncontrolled and controlled structure. Fig. 11 shows the time history of the base excitation, in which the peak ground acceleration (PGA) is 0.58g and the duration is 15 s. Figs. 12 and 13 show the time history of the roof displacement of the controlled and uncontrolled structure corresponding to $\xi_1 = 1\%$ and 2%, respectively. The maximum roof displacements of the uncontrolled building are 23.39 and 22.07 cm for these two cases, which are much greater than the 15 cm seismic joint. These results indicate that the building will impact its adjacent buildings while such an earthquake event occurs.

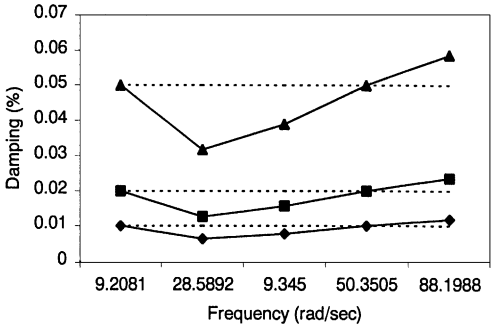

Fig. 10. Damping ratios for different modes.

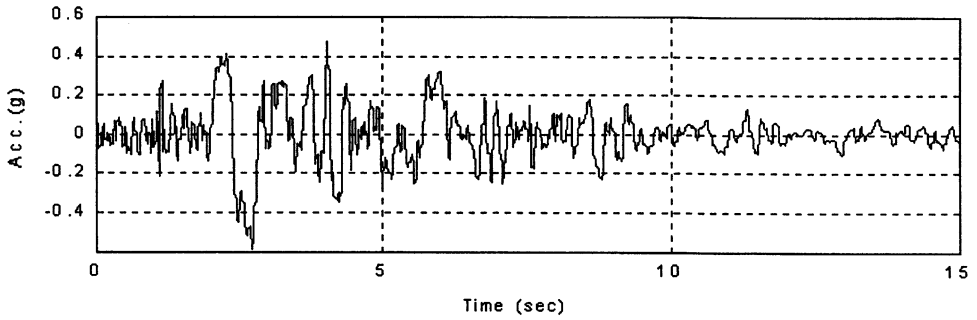

Fig. 11. Ground acceleration recorded at Rinaldi in 1994 during the Northridge Earthquake.

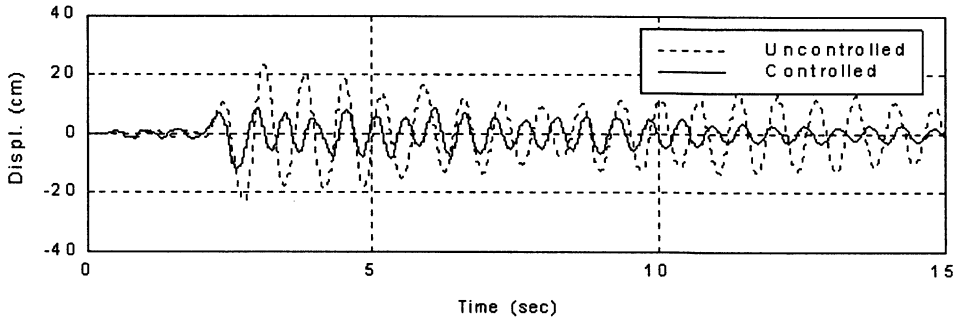

Fig. 12. Roof displacement (for $\xi_1 = 1\%$).

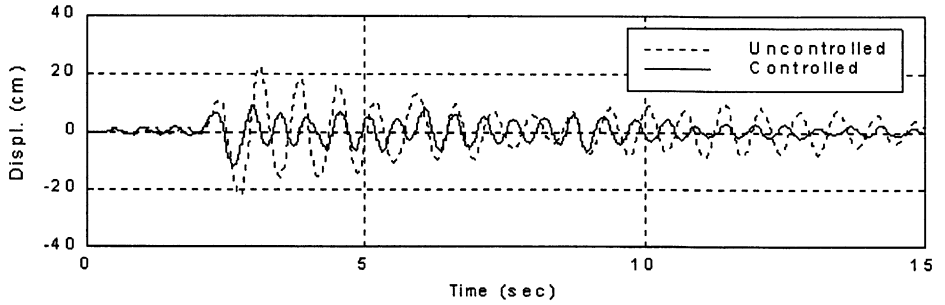

Fig. 13. Roof displacement (for $\xi_1 = 2\%$).

Assume the number of control forces is five and the same weight matrices **Q**, **R** as chosen in the Numerical example 2 are used in the control design for this building. The control feedback parameters are given as follows:

For $\xi_1 = 1\%$:

$$s_1 = 4.718 \times 10^3, \quad d_1 = 1.053 \times 10^4,$$
$$\mathbf{G}_1 = [422.4, 1328.4, 2108.0, 2707.4, 2927.3]^{\mathrm{T}},$$
$$\mathbf{G}_2 = [943.0, 2965.7, 4706.4, 6044.4, 6535.4]^{\mathrm{T}}. \tag{54}$$

Table 2
Roof displacement of the uncontrolled and controlled structure (cm)

Damping	Uncontrolled	Controlled	Reduction (%)	Force at roof (kN)
0.01	23.39	12.28	47.50	139.6
0.02	22.07	12.05	45.40	136.7

For $\xi_1 = 2\%$:

$$s_1 = 4.718 \times 10^3, \quad d_1 = 1.051 \times 10^4,$$
$$\mathbf{G}_1 = [422.4, 1328.4, 2108.0, 2707.4, 2927.3]^{\mathrm{T}},$$
$$\mathbf{G}_2 = [942.1, 2960.0, 4697.3, 6032.8, 6522.8]^{\mathrm{T}}. \tag{55}$$

It can be seen from Eqs. (54) and (55) that the effect of damping on the feedback matrices is not significant. Table 2 presents the peak values of the roof displacement of the controlled and uncontrolled structure corresponding to $\xi_1 = 1\%$ and 2%.

From Table 2, Figs. 11 and 12, it is clear that the roof displacement of the controlled structure has been reduced significantly and the variation of damping values in the structure does not affect the control effect when the active control is designed based on the proposed control algorithm. This practical example indicates that the proposed control algorithm is generally applicable to vibration control of civil engineering structures.

8. Conclusions

The effects of the modal control forces on the uncontrolled modes are examined for the IMSC algorithm. Theoretical analysis and numerical simulation study indicate that the contributions of the modal control forces to the response of the uncontrolled modes can be significant and cannot be neglected for some cases if the IMSC algorithm is used to design the structural control system. A new control algorithm—MIMSC has been proposed to eliminate the effects of the modal control forces. A numerical example is given for a six-story building first. Both the IMSC and MIMSC algorithms are used to design the control system for this structure. The numerical results indicate that the new algorithm is more efficient to control the structural vibration than the IMSC algorithm that may amplify the contributions of the uncontrolled modes to the structural responses. The computational results also show: (1) it is not necessary to examine the effects of the control forces to the higher modes if the control design is carried out based on the proposed algorithm, since such effects have been eliminated, (2) the contributions of the higher modes to the responses in the controlled structure are the same as those in the corresponding uncontrolled structure. However, the effects of the modal control forces on the uncontrolled modes should be carefully examined when the IMSC algorithm is used. In order to verify the effectiveness of the proposed algorithm, a practical example—active control design of UCLA Math-Science Building is presented and discussed. Numerical simulation has shown that the active control system designed by the proposed algorithm can reduce the structural response significantly, and the

variation of structural damping does not affect the control effect. Therefore, it is concluded that proposed control algorithm is generally applicable to vibration control of civil engineering structures.

Acknowledgements

The authors are thankful to the reviewers for their useful comments and suggestions. The work described in this paper was fully supported by a grant from the Research Grant Council of Hong Kong Special Administrative Region, China (Project No. CityU 1131/00E) and a grant from the City University of Hong Kong (Project No. 7100194).

Appendix A

$$\mathbf{\Phi} = \begin{bmatrix} 0.1327 & 0.3678 & -0.5178 & -0.5507 & 0.4565 & 0.2578 \\ 0.2578 & 0.5507 & -0.3678 & 0.1372 & -0.5178 & -0.4565 \\ 0.3678 & 0.4565 & 0.2578 & 0.5178 & 0.1327 & 0.5507 \\ 0.4565 & 0.1327 & 0.5507 & -0.2578 & 0.3678 & -0.5178 \\ 0.5178 & -0.2578 & 0.1327 & -0.4565 & -0.5507 & 0.3678 \\ 0.5507 & -0.5178 & -0.4565 & 0.3678 & 0.2578 & -0.1327 \end{bmatrix},$$

$\mathbf{K}^* = \mathrm{diag}(k_j^*)$,

$k_1^* = 0.0198 \times 10^9$, $k_2^* = 0.1712 \times 10^9$, $k_3^* = 0.4394 \times 10^9$, $k_4^* = 0.7629 \times 10^9$,

$k_5^* = 1.0675 \times 10^9$, $k_6^* = 1.2836 \times 10^9$,

$\mathbf{M}^* = \mathrm{diag}(m_j^*)$,

$m_j^* = m^* = 3.456 \times 10^5 \quad (j = 1, 2, \ldots, 6)$,

$\omega_1^2 = 57.2$, $\omega_2^2 = 495.4$, $\omega_3^2 = 1271.4$, $\omega_4^2 = 2207.4$, $\omega_5^2 = 3088.9$, $\omega_6^2 = 3714.2$,

$2\xi_1\omega_1 = 0.1513$, $2\xi_2\omega_2 = 0.6677$, $2\xi_3\omega_3 = 1.4263$, $2\xi_4\omega_4 = 2.3491$,

$2\xi_5\omega_5 = 3.3347$, $2\xi_6\omega_6 = 4.2261$.

Appendix B

Proposition. *When the control design is carried out based on the MIMSC algorithm, the following relation must be satisfied:*

$$m \geqslant R, \tag{B.1}$$

where m is the number of the control forces and R is the number of the controlled modes.

Proof. In the MIMSC, Eq. (36) must be held, then, one has

$$rank(\mathbf{H}\mathbf{G}_1) = rank(\mathbf{\Phi}^{\mathrm{T}}\mathbf{D}\mathbf{G}_1) = R, \tag{B.2a}$$

$$rank(\mathbf{H}\mathbf{G}_2) = rank(\mathbf{\Phi}^{\mathrm{T}}\mathbf{D}\mathbf{G}_2) = R, \tag{B.2b}$$

$rank(\mathbf{\Phi}^{\mathrm{T}}) = n$. Since $\mathbf{\Phi}^{\mathrm{T}}$ is a non-singular matrix, there are finite elementary matrices $\mathbf{L}_i$ $(i = 1, 2, \ldots, r)$ to make the following equation hold:

$$\mathbf{\Phi}^{\mathrm{T}} = \mathbf{L}_1\mathbf{L}_2\cdots\mathbf{L}_r, \tag{B.3}$$

therefore

$$\mathbf{\Phi}^{\mathrm{T}}\mathbf{D} = \mathbf{L}_1\mathbf{L}_2\cdots\mathbf{L}_r\mathbf{D}. \tag{B.4}$$

Because the rank of the matrix remains unchanged when it is multiplied by the elementary matrices, then

$$rank(\mathbf{\Phi}^{\mathrm{T}}\mathbf{D}) = rank(\mathbf{L}_1\mathbf{L}_2\cdots\mathbf{L}_r\mathbf{D}) = rank(\mathbf{D}) = m. \tag{B.5}$$

If $m < R$, then $rank(\mathbf{G}_1) = rank(\mathbf{G}_2) = m$, so that

$$rank(\mathbf{\Phi}^{\mathrm{T}}\mathbf{D}\mathbf{G}_1) = m < R, \tag{B.6a}$$

$$rank(\mathbf{\Phi}^{\mathrm{T}}\mathbf{D}\mathbf{G}_2) = m < R. \tag{B.6b}$$

Eqs. (B.2) are not satisfied, so as to $m \geqslant R$ must be satisfied, as claimed. □

References

[1] J.N. Yang, A. Akbarpour, P. Ghaemmaghami, New optimal control algorithms for structural control, Journal of Engineering Mechanics, American Society of Chemical Engineers 113 (9) (1987) 1369–1386.
[2] J.N. Yang, Z. Li, S.C. Liu, Instantaneous optimal control with velocity and acceleration feedbacks, Probabilistic Engineering Mechanics 16 (3) (1991) 204–211.
[3] J.N. Yang, Z. Li, S.C. Liu, Stable controllers for instantaneous optimal control, Journal of Engineering Mechanics, American Society of Civil Engineers 118 (8) (1992) 1621–1630.
[4] Q.S. Li, D.K. Liu, J.Q. Fang, Optimum design of actively controlled structures using genetic algorithms, Advances in Structural Engineering, An International Journal 2 (2) (1998) 109–118.
[5] Q.S. Li, H. Cao, G.Q. Li, S.J. Li, D.K. Liu, Optimal design of wind-induced vibration control of tall buildings and high-rise structures, Wind and Structures, An International Journal 2 (1) (1999) 69–83.
[6] Q.S. Li, D.K. Liu, J.Q. Fang, C.M. Tam, Multilevel optimal design of buildings with active control under winds using genetic algorithms, Journal of Wind Engineering and Industrial Aerodynamics 86 (1) (2000) 65–86.
[7] T.T. Soong, A.M. Reinhorn, Y.P. Wang, R.C. Lin, Full-scale implementation of active control. I: design and simulation, Journal of Structural Engineering, American Society of Civil Engineers 117 (11) (1991) 3516–3526.
[8] T.T. Soong, A.M. Reinhorn, Observed response of actively controlled structures, in: A.H.S. Ang, R. Villaverde (Eds.), Structural Engineering in Natural Hazard Mitigation, ASCE Press, New York, 1993, pp. 187–192.
[9] J.Q. Fang, The Design Theory and Method in Structural Control and Controlled Structures, Ph.D. Thesis, Wuhan University of Technology, PRC, 1993.
[10] L. Meirovitch, H. Oz, Active control of structures by modal synthesis, in: H.H. Leipholz (Ed.), Structural Control, North-Holland, Amsterdam, 1980, pp. 505–521.
[11] L. Meirovitch, H. Oz, Modal space control of distributed gyroscopic system, Journal of Guidance, Control and System 3 (1980) 140–150.
[12] T.T. Soong, Active Structural Control: Theory and Practice, Wiley, New York, 1990.

[13] M. Shinozuka, Digital simulation of random process and its applications, Journal of Sound and Vibration 25 (1) (1972) 111–128.
[14] G.C. Hart, J.Q. Fang, Earthquake response of the UCLA Math-Science building, Technical Report, Department of Civil and Environmental Engineering, UCLA, April, 1999.
[15] J.Q. Fang, Q.S. Li, A.P. Jeary, D.K. Liu, Damping of tall buildings: its evaluation and probabilistic characteristics, The Structural Design of Tall Buildings 8 (1999) 145–153.
[16] Q.S. Li, H. Cao, G.Q. Li, Analysis of free vibrations of tall buildings, Journal of Engineering Mechanics, American Society of Civil Engineers 120 (1994) 1861–1876.